European Journal of Pharmacology 933 (2022) 175287

Contents lists available at ScienceDirect

European Journal of Pharmacology

journal homepage: www.elsevier.com/locate/ejphar

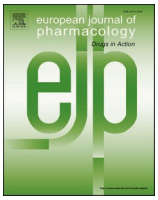

Inhibition of intraflagellar transport protein-88 promotes epithelial-to-mesenchymal transition and reduces cardiac remodeling post-myocardial infarction

Jessica N. Blom [a,1], Xiaoyan Wang [a,b,1], Xiangru Lu [a], Mella Y. Kim [a], Guoping Wang [b], Qingping Feng [a,c,*]

[a] Department of Physiology and Pharmacology, Schulich School of Medicine and Dentistry, Western University, London, Ontario, Canada
[b] Institute of Pathology, Tongji Hospital, Tongji Medical College, Huazhong University of Science and Technology, Wuhan, Hubei, China
[c] Department of Medicine, Schulich School of Medicine and Dentistry, Western University, London, Ontario, Canada

ARTICLE INFO

Keywords:
Primary cilium
Myocardial infarction
Epithelial-to-mesenchymal transition
Cardiac remodeling

ABSTRACT

The epicardium is a potential source of cardiac progenitors to support reparative angiogenesis after myocardial infarction (MI) through epithelial-to-mesenchymal transition (EMT). Primary cilia are recognized as hubs of cellular signaling, and their presence can alter downstream pathways to modulate EMT. The present study aimed to examine the effects of inhibiting intraflagellar transport protein-88 (Ift88), a protein vital to ciliary assembly, on epicardial EMT and cardiac remodeling post-MI. Epicardium derived cells (EPDCs) were cultured from E13.5 heart explants and treated with adenoviral vector encoding short-hairpin RNA against the mouse Ift88 (Ad-shIft88) to disassemble the primary cilium. Effects of Ad-shIft88 on epicardial EMT and cardiac remodeling were examined in mice post-MI. Our results show that Ad-shIft88 enhanced EMT of cultured EPDCs. In adult mice, intra-myocardial administration of Ad-shIft88 increased the number of Wilms tumor 1 (Wt1) positive cells in the epicardium and myocardium, promoted expression of genes associated with epicardial EMT, and enhanced capillary and arteriolar densities post-MI. Additionally, intra-myocardial Ad-shIft88 treatment attenuated cardiac hypertrophy and improved myocardial function three weeks post-MI. In conclusion, knockdown of Ift88 improves epicardial EMT, neovascularization and cardiac remodeling in the ischemic heart. Our study highlights the primary cilium as a potential therapeutic target post-MI.

1. Introduction

Ischemic heart disease is the leading global cause of death. After acute myocardial infarction (MI), a deleterious remodeling process takes place whereby the infarct expands, a fibrous collagen scar replaces lost myocardium, and the remaining viable cardiomyocytes hypertrophy in effort to compensate for the lost contractile tissue. This deleterious remodeling post-MI often causes heart failure, a deadly disease with a 5 year mortality of 60–75% (Bui et al., 2011). Despite the current available treatment options, heart failure remains a major cause of death and is a major economic burden globally (Cook et al., 2014).

Neovascularization in the infarct and peri-infarct area is critical to cardiac repair post-MI. The cardiac epicardium is involved in post-MI healing, and promotes angiogenesis and arteriogenesis for vascularization by secreting paracrine factors (Zhou et al., 2011; Xiang et al., 2014). Specifically, epicardium derived cells (EPDCs) are endogenous cardiac progenitors, which support coronary artery development during embryogenesis. During cardiogenesis, these epicardial cells begin to express the transcription factor Wilms tumor 1 (Wt1), and undergo the process of epithelial-to-mesenchymal transition (EMT) to invade the

Abbreviations: eGFP, enhanced green fluorescent protein; EMT, epithelial-to-mesenchymal transition; EPDC, epicardium derived cells; Ift88, intraflagellar transport protein-88; IP, intraperitoneal; MI, myocardial infarction; MOI, multiplicity of infection; PDGF, platelet-derived growth factor; PFU, plaque-forming unit; qPCR, quantitative polymerase chain reaction; TGFβ, transforming growth factor-beta; Wt1, Wilms tumor 1.

* Corresponding author. Department of Physiology and Pharmacology, Schulich School of Medicine and Dentistry, Western University, London, Ontario, N6A 5C1, Canada.
E-mail address: qfeng@uwo.ca (Q. Feng).

[1] Jessica N. Blom and Xiaoyan Wang contributed equally to this study.

https://doi.org/10.1016/j.ejphar.2022.175287
Received 5 June 2022; Received in revised form 6 September 2022; Accepted 13 September 2022
Available online 20 September 2022

myocardium and contribute perivascular and interstitial fibroblasts, epithelial cells and smooth muscle cells for vascularization (Smart et al., 2013). Typically, the adult epicardium is dormant; however, after MI, many epicardial cells express markers of embryonic progenitors, and are activated to undergo EMT and form EPDCs to promote neovascularization in the injured myocardium (von Gise and Pu, 2012; Blom and Feng, 2018). Unfortunately, this endogenous EPDC response is insufficient, and does not support adequate vascularization necessary for a complete functional recovery post-MI.

The primary cilium is an immotile specialized organelle protruding from the apical surface of most vertebrate cells (Blom and Feng, 2018). It is thought to integrate numerous sensory signaling pathways from extracellular signals, affectionately giving it the name the cellular "antenna". Included in the signaling pathways associated with the primary cilium are sonic hedgehog (Shh), wingless-type integration site (Wnt; canonical and non-canonical), and platelet-derived growth factor (PDGF), which are all integrated in the network related to EMT activation (Goetz and Anderson, 2010). Shh, Wnt and PDGF pathways support the loss of E-cadherin, gain of N-cadherin, and crosstalk with other pro-EMT mediators such as TGF-β (Gonzalez and Medici, 2014). Notably, disassembly of the primary cilium primes endothelial cells to shear stress-induced EMT during heart development (Egorova et al., 2011). Loss of the primary cilium also promotes EMT and metastatic invasion in numerous cancer cell types (Hassounah et al., 2012). Finally, in association with tissue wounding, TGF-β provokes deciliation along the wound edge, which incites EMT-type transitions (Rozycki et al., 2014). However, the effects of primary ciliary disassembly on epicardial EMT and angiogenesis post-MI are not known. Intraflagellar transport protein 88 (Ift88) is a transport protein required for both the assembly and structural maintenance of the primary cilium (Pazour et al., 2000). In the present study, we hypothesized that inhibition of *Ift88* using an adenoviral construct encoding a short hairpin RNA against Ift88 (Ad-shIft88) would potentiate primary cilia disassembly and improve EMT, myocardial neovascularization, and cardiac remodeling post-MI.

2. Materials and methods

2.1. Animals

All animals were handled in accordance with the guidelines of the Canadian Council on Animal Care and the use of animals was approved by the Animal Care Committee at Western University, London, Ontario, Canada (Approval number: AUP-2016-099).

2.2. Adenoviruses

To inhibit ciliary signalling, an adenoviral construct (Type 5 dE1E3) encoding a short-hairpin RNA against the mouse intraflagellar transport protein-88 (Ad-shIft88) (shRNA sequence: ccgg-gcaggaagactgaaagtga atctcgagattcactttcagtcttcctgc-tttttg) (Sanchez-Duffhues et al., 2015), driven by the human RNA polymerase III U6 promoter, and tagged with eGFP (cytomegalovirus promoter driven; CMV), was obtained from Vector Biolabs (Malvern, PA). An adenoviral construct containing CMV-driven green fluorescent protein (GFP) was used as control. Adenoviruses were propagated using HEK 293 cells, purified, and tittered using an AdEasy viral titer kit according to the manufacturer's instructions (Agilent Technologies, Santa Clara, CA).

2.3. Coronary artery ligation and in vivo adenoviral injection

Adult C57Bl/6 mice (males, 25–30 g of body weight, Charles River, Laval, Quebec, Canada) were anesthetized by ketamine (50 mg/kg, IP) and xylazine (12.5 mg/kg, IP). Animals were intubated and ventilated at a rate of 90 cycles per minute with a stroke volume of 0.34 mL (ventilation volume of 30.6 mL per minute) using a small animal ventilator (SAR 830, CWE Inc., Ardmore, Pennsylvania, USA). Myocardial infarction (MI) was induced by coronary artery ligation as described previously (Feng et al., 2001). For sham operations, a left thoracotomy was performed without left coronary artery ligation. The mice were randomly assigned to injections of either Ad-GFP or Ad-shIft88 (10^{10} PFU in 5 μL saline). Immediately after left coronary artery ligation, a total volume of 5 μL adenoviruses were injected intramyocardially into 3 sites (1.5–2 μL per site) in the peri-infarct area using a 30-gauge needle connected to a 25 μL Hamilton Gastight syringe (#3150801) via polyethylene (PE)10/PE50 tubing. The surgeon was blinded to the treatment groups. The thoracic cavity was closed using 8-0 sutures and mice were allowed to recover from the surgery. At day 3, 5 and 21 after sham or MI surgery, mice were re-anesthetized and hearts were collected. Adenoviral infection was confirmed by visualization of GFP fluorescence in heart sections; only those mice whose hearts expressed GFP upon visualization, indicating adenoviral infection, were used for subsequent analysis. Efficacy of Ad-shIft88 knockdown was assessed using RT-qPCR analysis of Ift88 mRNA levels 3-days post-MI.

Heart weight and body weight was recorded at the time of euthanasia. Infarct size of the adult heart was measured and expressed as a fraction of the total cross-sectional endocardial circumference (Feng et al., 2001). Finally, LV thickness, evaluated at the ventricular septum at the level of the suture was determined.

2.4. Echocardiography

Echocardiographic imaging was performed prior to surgery, as well as 21 days post-MI in adult mice using a Vevo 2100 ultrasound imaging system with a MS 400 transducer (VisualSonics, Toronto, Ontario) (Liu et al., 2014). Mice were anesthetized by inhalation of isoflurane with body temperature maintained at 37 °C. Cardiac functions were measured in both B and M mode with the probe positioned in long axis. Images were analyzed using Vevo Lab 3.1.1 analysis software.

2.5. Cell culture and adenovirus infection in vitro

Primary epicardium derived cells (EPDCs) were cultured as described previously (Liu et al., 2014; Moazzen et al., 2015). Briefly, fetal hearts at embryonic day 13.5 were dissected and ventricles were cut into four pieces. The ventricle pieces were plated on dishes in Dulbecco's modified eagle medium (DMEM) containing 10% fetal bovine serum. Epicardial cells migrated outward from the cardiac explant, forming a monolayer across the gelatin surface. After epicardial cells were grown outward for 7 days, EPDCs were trypsinized and re-plated for further experiments. Purity of EPDCs in culture was assessed by immunocytochemical staining using anti-mouse Wt1 (1:800, CA1026, lot 2786661, Calbiochem, San Diego, CA). For validation of Ift88 knockdown, first passage EPDCs were grown to confluence and treated with 10 multiplicity of infection (MOI) of Ad-shIft88 or Ad-GFP. After 48 h, medium containing virus was replaced with fresh serum-free medium for 24 h (Plotnikova et al., 2009; Ott and Lippincott-Schwartz, 2012). Cells grown on coverslips were then fixed and stained with acetylated α-tubulin primary antibody (1:2000, F6793, lot 034144828, Sigma-Aldrich, St. Louis, MO) to visualize cilia (Diguet et al., 2015). A minimum of 30 cells were examined for each culture using a fluorescent microscope (Observer D1, Zeiss, Germany) to quantify the cells containing a cilium, and measure the length of cilia. Cells grown in 24-well plates were used for analysis of Ift88 and E-cadherin mRNA levels by RT-qPCR.

2.6. EPDC EMT assay in vitro

Collagen (1 mg/ml, type I rat tail collagen, VWR CanLab) was solidified to a gel in 24-well plates and hydrated with OPTI-MEM media containing 1% FBS and insulin-transferrin-selenium (ITS) for 30 min at 37 °C. To determine the effect of ciliary disassembly on EMT, ventricles of E13.5 embryos were harvested as described above and plated on the

hydrated collagen gel (Lencinas et al., 2011; Moazzen et al., 2015). M199 medium (Sigma-Aldrich, St. Louis, MO) containing Ad-GFP or Ad-shIft88 (10 MOI) was then added to the culture. After three days, the number of spindle shaped cells grown outward from the explanted ventricles was quantified. Images were captured using phase contrast microscope (Observer D1, Zeiss, Germany).

2.7. Histological analysis

Hearts were fixed in 4% paraformaldehyde at 4 °C overnight, dehydrated in ethanol, and paraffin embedded. Each heart was cut into 5 μm sections (Leica RM2255 microtome) and mounted on positively charged micro slides. All images for histological analysis were obtained using a light microscope and Axiocam ICc 5 camera (Zeiss, Germany). Cardiac tissue sections from adult mice 21 days post-MI were stained with hematoxylin and eosin (H/E) for analysis of myocyte cell size (Xiang et al., 2009). Myocyte diameter was measured as shortest cross sectional diameter at nuclei level in a minimum of 5 sections and 50 cells per heart.

2.8. Immunohistochemical analysis

To show GFP and Wt1 positive cells, heart sections were immunostained using rabbit anti-GFP polyclonal IgG (1:500, AB290, lot GR3222604, Abcam, Cambridge, MA) and rabbit anti-mouse Wt1 (1:800, CA1026, lot 2786661, Calbiochem, San Diego, CA) following antigen retrieval in citrate buffer 10 mM pH 6.0 for 12 min at 94 °C using a microwave oven (BP-111; Microwave Research & Applications, Inc., Carol Stream, IL) (Xiang et al., 2014). To quantify capillary abundance, heart sections were stained with biotinylated *Griffonia (Bandeiraea) simplicifolia* lectin I (1:200, B1105, Vector Laboratory, Burlingame, CA). Arteriole abundance was analyzed by staining smooth muscle cells with α-smooth muscle actin (α-SMA; 1:1000, A2547, lot 032M4822, Sigma-Aldrich, St. Louis, MO). Primary antibodies for Wt1 and α-SMA were followed by goat anti-rabbit IgG secondary antibody (1:500, SC-2018, lot I0514, Santa Cruz, Dallas, TX) and rabbit anti-mouse IgG secondary antibody (1:500, BA9200, Vector Laboratories, Burlingame, CA) respectively. All signals were visualized using avidin and biotinylated HRP (Santa Cruz) followed by 3-3'diaminobenzidine tetrahydrochloride (Sigma-Aldrich St. Louis, MO). Nuclei were counterstained with modified Mayer's hematoxylin (Thermo Scientific, Waltham, MA). The abundance of positive signal was analyzed in at least 5 individual heart sections per sample, and at least 4 fields in each section. For Wt1, arteriole abundance, and capillary abundance, positive cells/vessels were quantified and normalized to the myocardial area (Xiang et al., 2014).

2.9. Real-time qPCR

Total RNA from cultured EPDCs and peri-infarct area of hearts three days post-MI was isolated using Trizol reagent (Ambion, Foster City, CA). Moloney murine leukemia virus (M-MLV) reverse transcriptase was used to synthesize cDNA (from a minimum total RNA of 0.35 μg for cells and 0.55 μg for tissues) in 20 μL reactions. EvaGreen qPCR MasterMix-S (ABM, Vancouver, BC) was used for real-time PCR amplification with 2 μL cDNA, as per the manufacturer's instructions. Samples were amplified for 35 cycles using Eppendorf Realplex^2 Real-time qPCR machine and analyzed using cycle threshold (Ct) analysis. Primer sequences for expression analysis are listed in Table 1. The mRNA levels in relation to murine glyceraldehyde 3-phosphate dehydrogenase (*GAPDH*) or 28S ribosomal RNA as an internal control were determined using a comparative C_T method (Moazzen et al., 2020).

2.10. Statistical analysis

Data are means ± SEM. A one- or two-way ANOVA followed by a Bonferroni test was performed for multiple group comparisons (GraphPad Prism software, version 9.1). An unpaired Student's t-test was used to detect significance between two groups. All tests were two sided, using a significance level of $P<0.05$.

Table 1
Real-time qPCR primer sequences.

Gene	Accession #	Forward (5′-3′)	Reverse (5′-3′)
Ift88	NM_009376	gcgtttcttggttcgtctct	cactcccctctcgtttgct
Snail1	NM_011427.2	cacacgctgccttgtgtct	ggtcagcaaaagcacggtt
Slug	NM_011415.2	caacgcctccaagaagccca	gagctgccgacgatgtccat
β-Catenin	NM_001165902	cttggctgaaccatcacagat	agcttcctttttggaaagctg
Wnt1	NM_021279	ctggaactgccccactgct	gccaaagaggcgaccaaaat
Tbx18	NM_023814	gagcagcaacccgtctgtga	gggactgtgcaatcggaagg
Hif-1α	NM_001313919	cagcctcaccagacagagca	gtgcacagtcacctggttgc
bFGF	NM_008006	caagggagtgtgtgccaacc	tgcccagttcgtttcagtgc
Tgf-β1	NM_011577	gcccgaagcggactactatg	cactgcttcccgaatgtctg
E-Cadherin (Cdh1)	NM_009864	actgtgaagggacggtcaac	ggagcagcaggatcagaatc
GAPDH	NM_001289726	gatgggtgtgaaccacgaga	Agtgatggcatggactgtgg
28S	NR_003279.1	gggccacttttggtaagcag	ttgattcggcaggtgagttg

3. Results

3.1. Effects of Ad-shIft88 on primary cilia disassembly and epicardial EMT

To assess primary cilia disassembly, EPDCs isolated from the outgrowth of E13.5 mouse heart explants were grown on gelatin coated 24-well plates and treated with Ad-shIft88 or adenoviral constructs encoding green fluorescence protein (Ad-GFP, 10 MOI). Two days after treatment, cells were changed to serum free medium, to elucidate the presence of primary cilia. Treatment with Ad-shIft88 significantly reduced *Ift88* transcript levels compared to Ad-GFP treated cells, as measured by real time RT-qPCR ($P<0.05$, Fig. 1A). Additionally, a significant reduction in *E-cadherin* (*Cdh1*) mRNA levels, a marker of EMT, was observed ($P<0.05$, Fig. 1B). Notably, the primary cilium was revealed in cultured EPDCs using immunostaining of acetylated α-tubulin (Fig. 1C). Ad-shIft88 treatment significantly reduced the ciliary length ($P<0.01$, Fig. 1D) as well as the percent of ciliated cells ($P<0.05$, Fig. 1E).

To investigate whether Ift88 knockdown promotes epicardial EMT, E13.5 mouse hearts were cultured on a collagen gel to allow epicardial cell outgrowth and EMT to become spindle shaped cells (Potts and Runyan, 1989). The number of spindle shaped cells was quantified and normalized to the heart explant area. Ad-shIft88 treated cultures had a significantly higher number of spindle shaped EPDCs as compared to Ad-GFP controls ($P<0.05$, Fig. 1F and G). These data indicate that Ift88 knockdown promotes EMT of epicardial cells.

3.2. Effects of Ad-shIft88 on epicardial activation and growth factor release post-MI

To assess *in vivo* adenoviral transduction efficiency, GFP immunostaining was performed in hearts 3 days after MI and peri-infarct administration of Ad-GFP or Ad-shIft88 with an eGFP tag. Our data show that the epicardium was strongly positive for GFP in both Ad-GFP and Ad-shIft88 treated hearts (Fig. 2A), indicating an excellent adenoviral transduction efficiency in the epicardium. Within the peri-infarct myocardium, strong GFP staining was seen in cardiomyocytes at 5 and 21 days post-MI after Ad-shIft88 injections (Supplementary Figs. 1A and B). Vascular smooth muscle cells in coronary vessels were also positive for GFP (Supplementary Fig. 1A).

To assess epicardial activation and EMT induced by Ad-shIft88, adult mice were subjected to coronary artery ligation to induce MI, and epicardial and myocardial expression of Wt1, a marker of epicardial activation and EMT, was assessed by immunohistochemistry 3 days

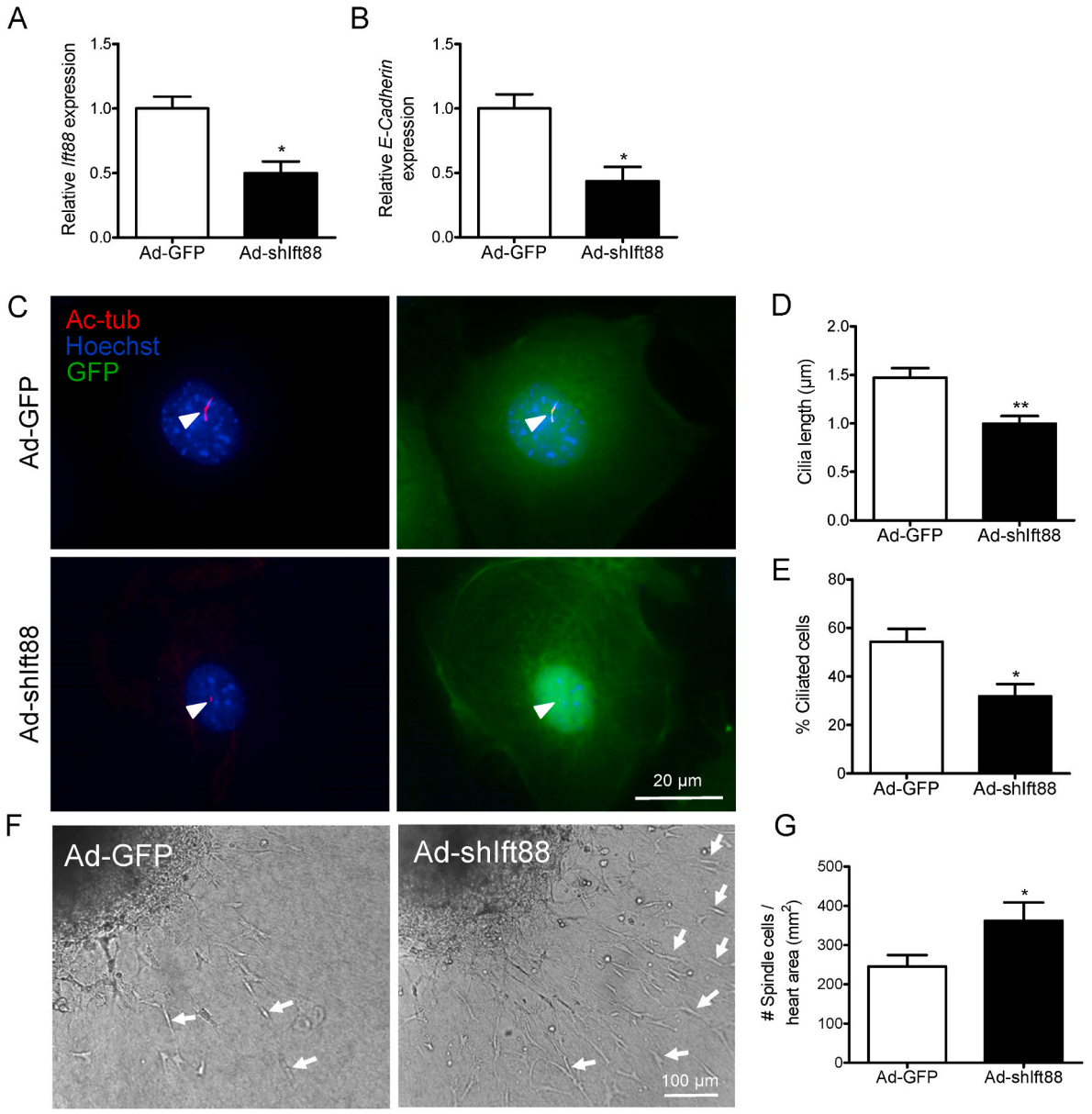

Fig. 1. Effects of Ad-shIft88 on epicardial EMT. Epicardium derived cells (EPDCs) isolated from E13.5 heart explants were grown on a gelatin-coated dish. Cells were treated with adenoviral constructs encoding a short hairpin RNA against intraflagellar transport protein-88 (Ad-shIft88) or green fluorescence protein (Ad-GFP, 10 MOI) for 48 h followed by 24 h serum starvation. (A and B) *Ift88* and *E-Cadherin* mRNA levels measured by real-time qPCR. (C) Representative images of EPDCs stained with acetylated α-tubulin (red; white arrow heads). Adenoviral infections are indicated by GFP expression (green). (D) Cilia length. (E) Percentage of cells with the primary cilium longer than 1.5 μm. (F) E13.5 heart explants were cultured on collagen coated dishes with Ad-GFP or Ad-shIft88 (10 MOI) treatment. Epicardial cells that have undergone EMT are spindle shaped (white arrows). (G) Three days post-treatment the number of spindle shaped cells (the cells that have undergone EMT) was quantified. Data are mean ± SEM from 3 (A–E) and 9 (G) independent experiments. *$P<0.05$, **$P<0.01$ vs. Ad-GFP.

post-MI (Fig. 2B). Quantitative analysis demonstrated that there were significantly more Wt1 positive cells on the epicardium and in the myocardium of the peri-infarct area in Ad-shIft88 treated mice compared to Ad-GFP treated mice post-MI ($P<0.05$, Fig. 2C and D).

Ift88 knockdown was confirmed by real-time RT-qPCR 3 days post-surgery; treatment with Ad-shIft88 significantly reduced myocardial Ift88 mRNA levels in both sham and MI mice as compared to Ad-GFP treated hearts ($P<0.05$, Fig. 3A). To further understand the effect of Ad-shIft88 on EMT in the peri-infarct area post-MI, expression of key molecular regulators of EMT was assessed by RT-qPCR. *Tbx18* is an epicardial transcription factor enriched in the embryonic heart, and marks epicardial activation after injury. *Tbx18* has been shown to upregulate *Snail* and *Slug* expression, which are involved in EMT and critically modulate *E-cadherin* expression (Takeichi et al., 2013; Jing et al., 2016). *Wnt1* and *β-catenin* are also critical to EMT and aid in epicardial activation via both canonical Wnt (β-catenin-dependent) and non-canonical Wnt signaling (β-catenin-independent) (Duan et al., 2012). Importantly, *Tbx18, Snail, Slug, Wnt1,* and *β-catenin* are all known to be expressed by transitioning EPDCs. Ad-shIft88 treatment significantly increased the mRNA expression of *Tbx18*, *Snail, Slug, Wnt1,* and *β-catenin* in the peri-infarct area post-MI ($P<0.05$, Fig. 3B–F). Additionally, hypoxia-inducible factor 1-alpha (HIF-1α) is a master regulator of vasculogenesis, which induces growth factors to provoke both EMT and blood vessel development (Tao et al., 2013). The mRNA levels of *HIF-1α* and basic fibroblast growth factor (*bFGF*) were significantly higher in the Ad-shIft88 treated group as compared to controls ($P<0.05$, Fig. 3G and H). Finally, EMT of EPDCs is regulated by TGF-β (Bax et al., 2011), which was also upregulated in the Ad-shIft88 treated group

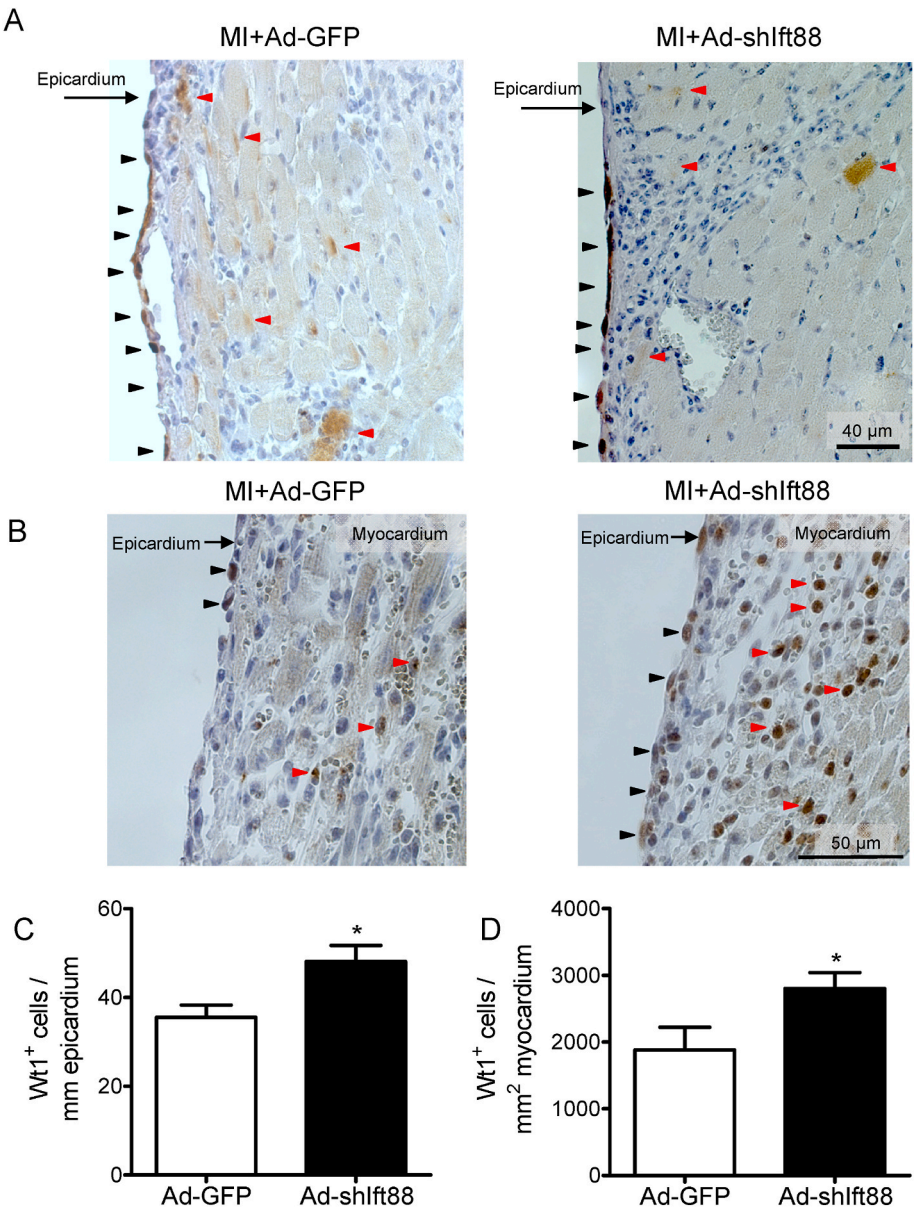

Fig. 2. Effects of Ad-shIft88 on Wt1 expression in the peri-infarct area post-MI. Adult mice were subjected to MI by coronary artery ligation and treated with either Ad-GFP or Ad-shIft88 (10^{10} PFU) intramyocardially in peri-infarct area. Hearts were collected 3 days post-MI. Representative immunostaining images of GFP (A) and Wilms tumor 1 (Wt1, B) using respective antibodies. Positive cells show brown or dark brown staining. Black arrow heads point to GFP (A) and Wt1 (B) positive cells in the epicardium, and red arrow heads point to GFP or Wt1 positive cells in the myocardium. Quantification of Wt1 positive cells in the epicardium (C) and myocardium (D) of the peri-infarct area. Data are mean ± SEM, n = 8–9 mice per group. *P<0.05 vs. MI + Ad-GFP.

(P<0.05, Fig. 3I). Together, these results indicate that Ad-shIft88 enhances the expression of transcription and growth factors that promote epicardial EMT post-MI.

3.3. Effects of Ad-shIft88 on capillary and arteriolar density post-MI

EPDCs are essential for the development of the coronary vasculature (Perez-Pomares and de la Pompa, 2011). Given the observed increase in EPDC activation post-MI, we hypothesized that Ad-shIft88 treatment would augment angiogenesis in the peri-infarct region. To test this hypothesis, lectin staining was employed to specifically stain endothelial cells and quantify myocardial capillary density (Fig. 4A). At 5 days post-MI, myocardial capillary density was higher in the Ad-shIft88 treated group as compared to the Ad-GFP treated group (P<0.05, Supplementary Figs. 2A–C). Notably, a significant increase in capillary density was seen at 21 days post-MI (P<0.05, Fig. 4A–B).

In addition to angiogenesis, EPDCs have been shown to promote arteriogenesis (Xiang et al., 2014). To determine whether enhanced epicardial activation affected arteriogenesis in the peri-infarct region, α-SMA staining was employed to stain smooth muscle cells (Fig. 4C). The number of arterioles (between 10 and 150 μm in diameter) in the peri-infarct area 5 days post-MI was quantified. Arteriole density was significantly higher in Ad-shIft88 treated hearts as compared to Ad-GFP treated hearts (P<0.05, Supplementary Figs. 2D–F). This difference was maintained to 21 days post-MI (P<0.05, Fig. 4C–D). These data show that Ift88 knockdown promotes myocardial neovascularization post-MI.

3.4. Effects of Ad-shIft88 on cardiac hypertrophy post-MI

Cardiac hypertrophy is indicative of detrimental remodeling post-MI and can be assessed by the heart weight/body weight ratio and the thickness of the ventricular septum. To determine whether Ift88 knockdown affects cardiac hypertrophy, adult mice were subjected to sham or MI surgery with Ad-GFP or Ad-shIft88 treatment. Our data show that infarct size and body weight were similar between Ad-GFP and Ad-shIft88 treated mice at 21 days post-MI (P=n.s., Fig. 5A and B). However, the heart weight/body weight ratio and ventricular septal thickness were significantly higher in MI mice treated with Ad-GFP compared to sham-operated controls, and both parameters were significantly reduced by Ad-shIft88 treatment (P<0.05, Fig. 5C and D). To further

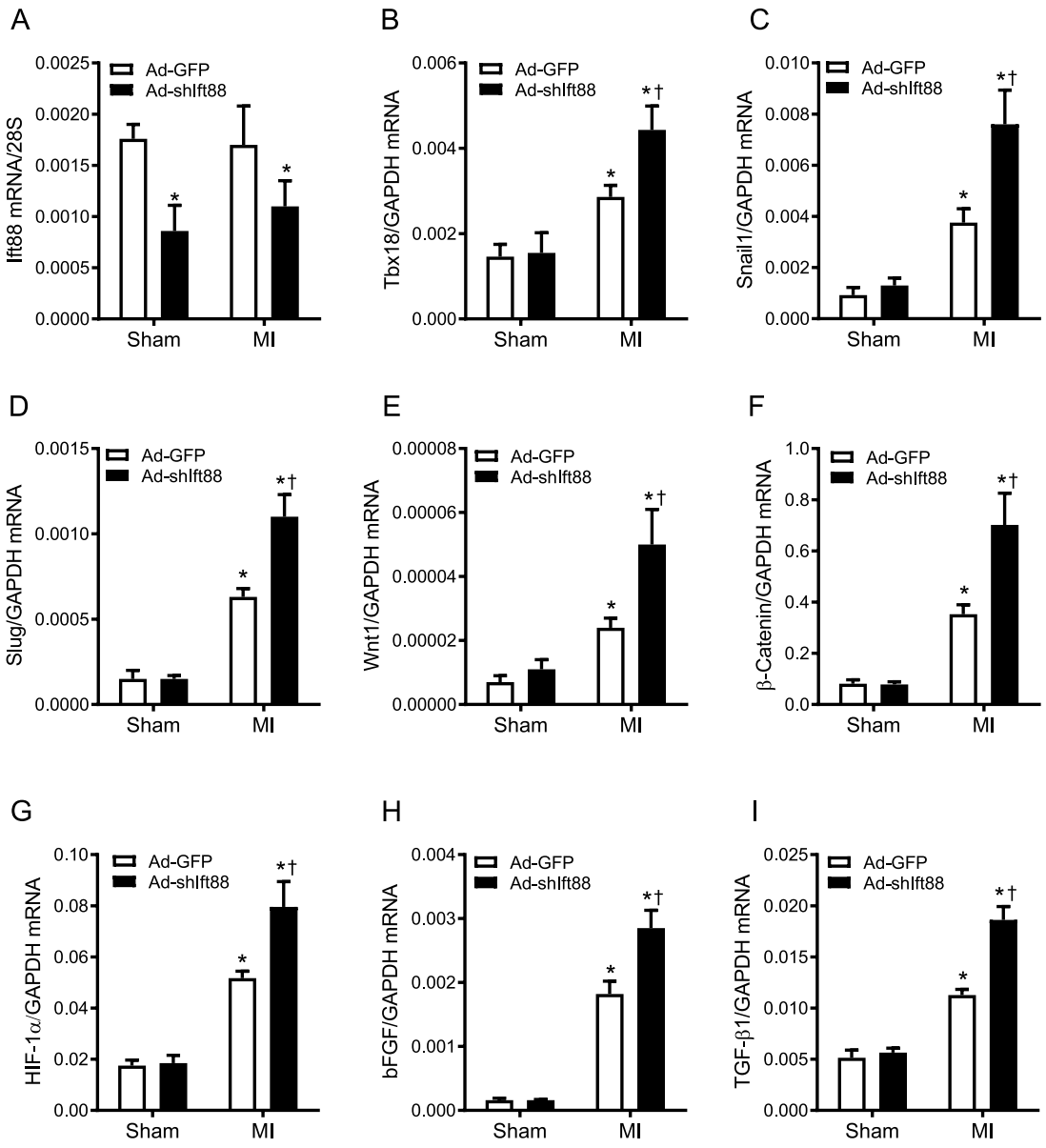

Fig. 3. Effects of Ad-shIft88 on myocardial expression of EMT markers and growth factors post-MI. Adult mice were subjected to MI by coronary artery ligation and injected with either Ad-GFP or Ad-shIft88 (10^{10} PFU) intramyocardially in the peri-infarct area. Tissues from the peri-infarct area were collected 3 days post-MI. mRNA levels were analyzed by real-time qPCR for *Ift88* (A), *Tbx18* (B), *Snail* (C), *Slug* (D), *Wnt1* (E), *β-Catenin* (F), *HIF-1α* (G), *bFGF* (H), and *TGF-β1* (I). Data are mean ± SEM, n = 6 mice per group. *$P<0.05$ vs. Sham + Ad-GFP. †$P<0.05$ vs. MI + Ad-GFP.

assess cardiac hypertrophy, cardiomyocyte cell size in the peri-infarct area was examined by measuring the minimum cross-sectional transverse diameter at the nuclear level of cardiomyocytes in hematoxylin/eosin-stained heart sections (Xiang et al., 2009). Treatment with Ad-shIft88 significantly lowered cardiomyocyte cross-sectional diameter as compared to the Ad-GFP treated group ($P<0.05$, Fig. 5E and F).

3.5. Effects of Ad-shIft88 on cardiac function post-MI

Cardiac function was assessed by echocardiography and the parameters are presented in Table 2. MI significantly reduced stroke volume (SV), cardiac output (CO), left ventricular ejection fraction (LVEF) and fractional shortening (LVFS) compared to sham-operated controls ($P<0.01$). Treatment with Ad-GFP or Ad-shIft88 had no significant effects on cardiac function in sham-operated mice. Ad-GFP treatment did not significantly alter cardiac function post-MI. Notably, Ad-shIft88 treatment significantly improved SV, CO, LVEF and LVFS in MI mice compared to the Ad-GFP treatment group (Table 2, $P<0.05$). These data show that Ad-shIft88 treatment improves cardiac function post-MI.

4. Discussion

The present study has demonstrated a novel role for the primary cilium in modulating epicardial activation and neovascularization post-MI. Our data show that knockdown of the required ciliary transport protein Ift88 promotes EMT and neovascularization post-MI, reduces the deleterious remodeling process and improves cardiac function 3 weeks after MI. These data suggest that primary ciliary disassembly affects epicardial EMT and cardiac remodeling in the ischemic heart. We have previously demonstrated the ability of Wt1 positive EPDCs to migrate into the infarct and peri-infarct area post-MI to contribute to neovascularization (Xiang et al., 2014). However, this endogenous

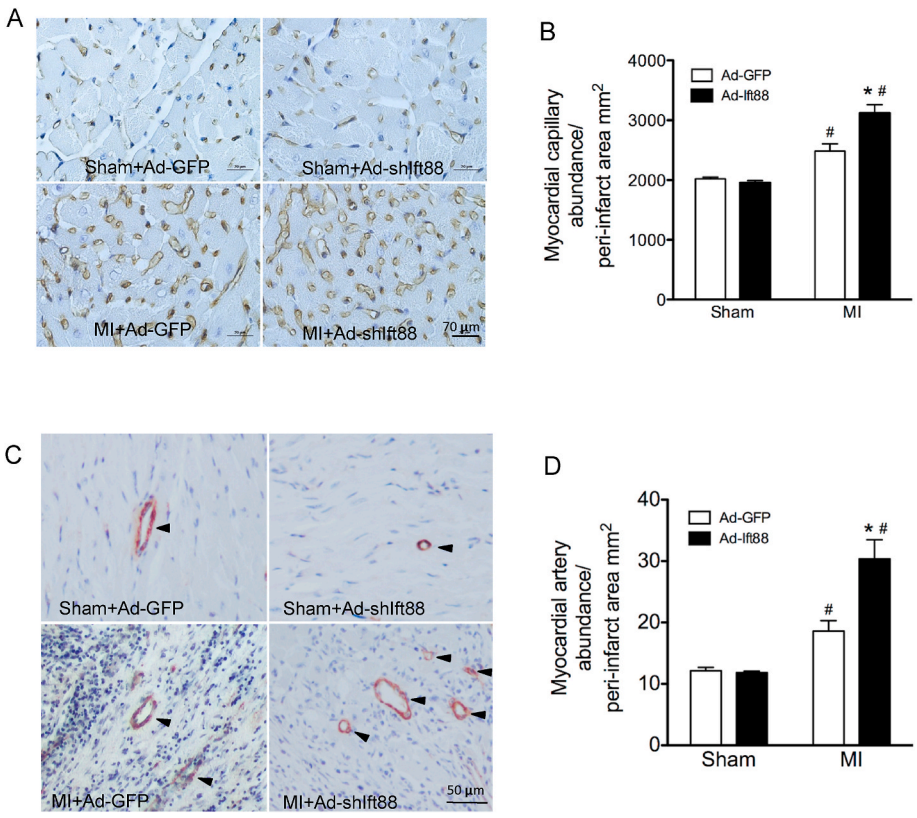

Fig. 4. Effects of Ad-shIft88 on myocardial capillary and arteriolar density in the peri-infarct area post-MI. Adult mice were subjected to MI by coronary artery ligation and treated with either Ad-GFP or Ad-shIft88 (10^{10} PFU) in the peri-infarct area. (A) Representative images of lectin staining (brown). (B) Quantification of capillary density in the peri-infarct area 21 days post-MI. (C) Representative images of α-SMA staining. Arterioles were identified as small vessels 10–150 μm in diameter surrounded by α-SMA positive cells. Black arrows indicate arterioles. (D) Quantification of arteriole density in the peri-infarct area 21 days post-MI. Data are mean ± SEM, n = 8–9 mice per group for day 21. *P<0.05 vs. Sham + Ad-GFP. †P<0.05 vs. MI + Ad-GFP.

activation is not enough to completely salvage the ischemic myocardium post-MI. It is likely that the enhanced Wt1 expression in the epicardium and myocardium in the Ad-shIft88 treated hearts in the present study is indicative of increasing numbers of EPDCs that have migrated into the myocardium. Notably, this response improves neovascularization, a hypothesis supported by our observation of increased capillary and arteriolar densities in the peri-infarct area in the Ad-shIft88 treated mice. Furthermore, Ad-shIft88 treatment significantly attenuated hypertrophic response, which typically contributes to the cardiac remodeling leading to heart failure.

Interestingly, primary cilia are required for proper situs during development, and mutations in ciliary proteins cause congenital heart defects (Li et al., 2015). Specifically, the primary cilium cannot endure high levels of shear stress, and the loss of cilia primes the endocardium to shear-stress induced endothelial-to-mesenchymal transition, which is critical to endocardial cushion formation and compact myocardium development (Egorova et al., 2011). Slough et al. demonstrated the presence of cilia on the epicardium (Slough et al., 2008). Here we confirm that mouse epicardial cells are indeed ciliated, and that loss of the primary cilium supports a transition from an epithelial phenotype to a mesenchymal phenotype of epicardial cells.

Primary cilia are known to modulate Wnt, Shh, and PDGF signalling, and have recently been demarcated as an important site moderating TGF-β mediated responses (Bodle and Loboa, 2016; Blom and Feng, 2018). Interestingly, TGF-β alone without deciliation is not sufficient to cause EMT in tubular epithelial cells (Rozycki et al., 2014). While the EMT effects of Wnt, Shh and PDGF have been established in epicardial cells after cardiac injury (Kim et al., 2010; Duan et al., 2012; Wang et al., 2015), the role of primary cilia in these cells post-MI is not known. In the present study, the effects of primary cilia disassembly on these EMT pathways were highlighted demonstrating an increased expression of their molecular mediators, including *β-catenin, Snail,* and *Slug,* after Ad-shIft88 treatment post-MI. The finding of enhanced Wnt/β-catenin activity is particularly noteworthy given the well-established role of β-catenin in mediating EMT (Valenta et al., 2012). The primary cilium dampens the canonical Wnt pathway by diverting Jouberin (Jbn), a context specific Wnt regulator, away from nucleus and limits β-catenin nuclear entry through regulated intraflagellar transport (Lancaster et al., 2011; Blom and Feng, 2018). Additionally, β-catenin mediated upregulation of Slug has been demonstrated to be responsible for mesenchymal transformation of aortic endothelial cells lacking primary cilia (Sanchez-Duffhues et al., 2015).

In the present study, adenoviral mediated shRNA delivery was used to knockdown the Ift88 transport protein. Using this approach, we observed EMT in cultured epicardial cells. Furthermore, treatment with Ad-shIft88 *in vivo* promotes epicardial EMT as indicated by increases in the number of $Wt1^+$ cells in the epicardium and myocardium associated with higher *Snail* and *Slug* expression. Notably, fetal cardiomyocytes are ciliated (Zebrowski et al., 2015). Shortly after birth, the centrosome, a juxtanuclear organelle critical to primary cilium formation, is lost in cardiomyocytes, making them unable to undergo ciliogenesis. The loss of centrosome integrity is associated with deciliation, cell cycle arrest and post-mitotic state in postnatal rat cardiomyocytes (Zebrowski et al., 2015). In the adult mouse and human hearts, cardiac fibroblasts, but not cardiomyocytes, are ciliated, and the primary cilia are required for TGFβ1-induced fibrogenesis (Myklebust et al., 1977; Villalobos et al., 2019). Additionally, deficiency in Alstrom syndrome protein 1 (ALMS1), which is localized to centrosomes and the base of primary cilia, has been shown to impair terminal differentiation but promote proliferation of postnatal cardiomyocytes (Shenje et al., 2014). Since cardiomyocytes are nonciliated after birth, these effects in the Alms1 mutant mice are likely independent of primary ciliary disassembly. In the present study, treatment with Ad-shIft88 did not significantly alter the number of proliferating cells in the peri-infarct area (data not shown), suggesting the observed effects are not a result of enhanced cell proliferation in the heart post-MI.

A major limitation of our study is that the specific role of epicardial cells in mediating the beneficial effects of Ad-shIft88 in mice post-MI

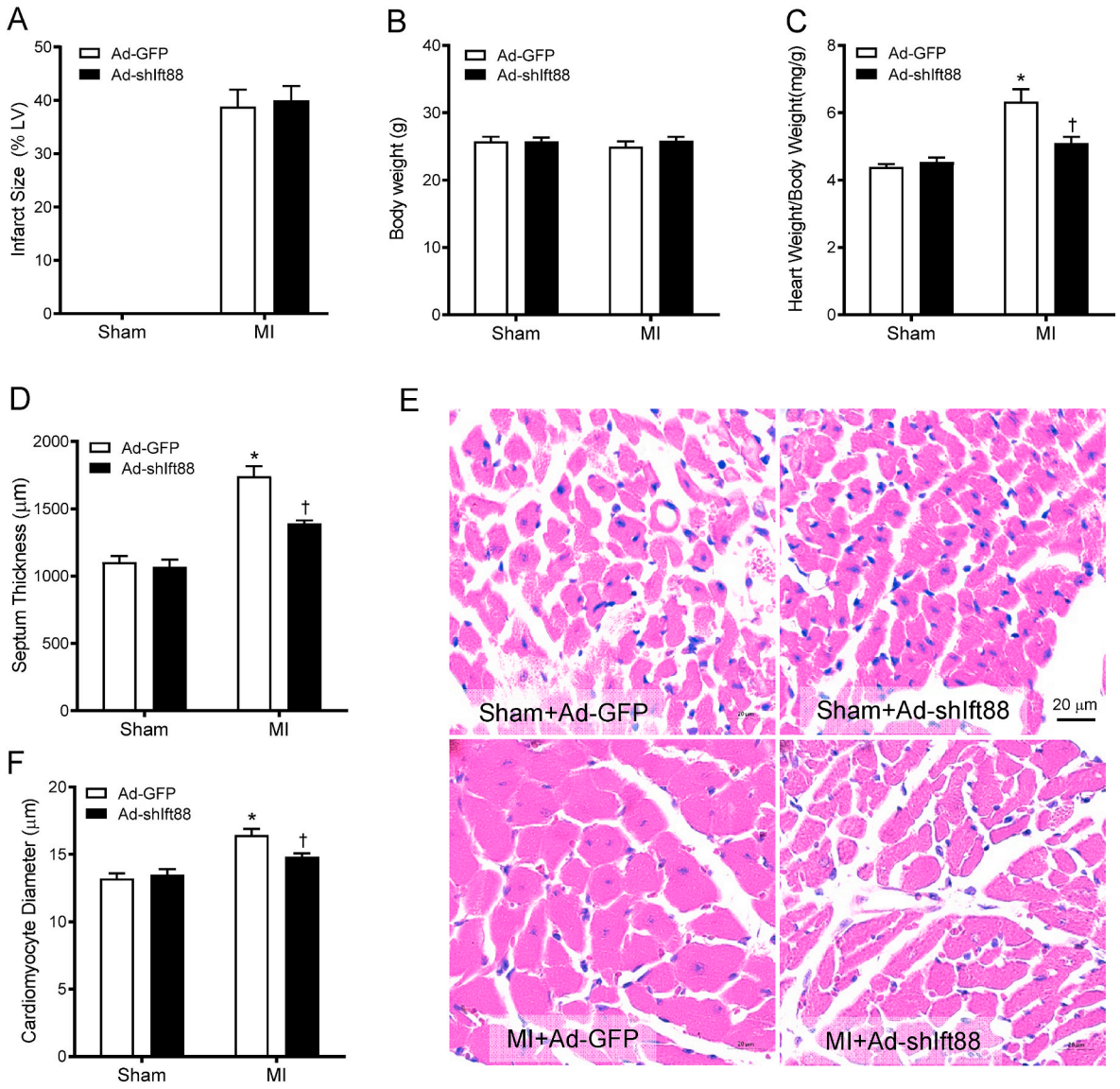

Fig. 5. Effects of Ad-shIft88 on cardiac hypertrophy 21 days post-MI. Adult mice were subjected to MI by coronary artery ligation and injected with either Ad-GFP or Ad-shIft88 (10^{10} PFU) in the peri-infarct area. Infarct size (A), body weight (B), heart weight to body weight ratio (C), septal myocardium thickness (D), and cardiomyocyte cell size (E and F) were assessed at 21 days post-MI. (E) Representative photomicrographs of hematoxylin- and eosin-stained sections showing cross-sections of cardiomyocytes. (F) Analysis of cardiomyocyte cross-sectional diameter. Data are mean ± SEM, n = 8–10 mice per group. *$P<0.05$ vs. Sham + Ad-GFP. †$P<0.05$ vs. MI + Ad-GFP.

was not determined. Other cell types in the heart including endocardial cells, endothelial cells and fibroblasts also possess primary cilia. It is possible that Ad-shIft88 treatment may induce ciliary disassembly and EMT of these cells in the infarcted heart. Notably, endothelial EMT has been shown to promote cardiac fibrosis (Murdoch et al., 2014). On the other hand, ciliated fibroblasts are enriched in areas of myocardial injury and depletion of the primary cilia in cardiac fibroblasts reduces collagen production in response to TGFβ1 stimulation (Villalobos et al., 2019). While fibrosis is required for infarct healing in the acute phase of MI, long-term cardiac fibrosis causes cardiac remodeling and impairs cardiac function. Thus, disassembly of the primary cilia of cardiac fibroblasts may reduce cardiac fibrosis and remodeling after acute MI. Whether cardiac fibroblasts are targeted by Ad-shIft88 treatment in the infarcted myocardium merits further investigation.

5. Conclusion

The present investigation showed that intra-myocardial Ad-shIft88 treatment to induce primary cilia disassembly promotes epicardial EMT and potentiates Wnt/β-catenin and growth factor (bFGF) expression, improving myocardial neovascularization, cardiac remodeling and function post-MI. Our study uncovers the importance of primary cilia in cardiac remodeling and highlights the primary cilium as a possible therapeutic target post-MI although the specific cell type responsible for the beneficial effects remains to be determined.

CRediT authorship contribution statement

Jessica N. Blom: conceived the experiments. designed the experiments. performed the experiments and data analyses. wrote the manuscript. revised the manuscript. **Xiaoyan Wang:** designed the experiments. performed the experiments and data analyses. revised the manuscript. **Xiangru Lu:** conceived the experiments. designed the experiments. performed the experiments and data analyses. revised the manuscript. **Mella Y. Kim:** performed the experiments and data analyses. **Guoping Wang:** involved in experimental design and revised the

Table 2
Effects of intra-myocardial treatment of Ad-GFP and Ad-shIft88 on echocardiographic parameters of mice 21 days after sham or MI surgery.

Parameters	Sham		MI	
	Ad-GFP	Ad-shIft88	Ad-GFP	Ad-shIft88
n	7	6	8	7
HR (beats/min)	516.9 ± 15.8	518.7 ± 6.1	487.0 ± 8.1	484.2 ± 24.5
LV Area;s (mm^2)	14.1 ± 1.2	14.7 ± 1.2	32.2 ± 3.6*	29.9 ± 1.9
LV Area; d (mm^2)	26.8 ± 1.0	26.7 ± 1.7	35.5 ± 3.6*	37.3 ± 2.1
LV Vol;s (μl)	28.7 ± 4.8	31.3 ± 4.1	117.7 ± 22.4*	102.4 ± 10.1
LV Vol;d (μl)	78.9 ± 5.6	78.8 ± 8.1	134.5 ± 23.0*	140.0 ± 10.1
SV (μl)	50.2 ± 3.2	47.5 ± 4.5	17.23 ± 1.2**	37.7 ± 2.5†
CO (ml/min)	25.8 ± 1.6	25.9 ± 2.4	8.2 ± 0.6**	18.0 ± 1.0††
LVEF (%)	64.5 ± 3.7	60.8 ± 2.0	14.3 ± 1.4**	27.7 ± 2.9†
LVFS (%)	23.9 ± 1.0	24.3 ± 2.1	3.6 ± 0.4**	10.5 ± 0.2††

Adult mice were subjected to MI by coronary artery ligation and treated with Ad-GFP or Ad-shIft88 (10^{10} PFU) in the peri-infarct area. Echocardiography was performed at 21 days post-surgery with adenovirus treatment. HR, heart rate. Area; s and Area; d are area of left ventricle (LV) at the end of systole and diastole, respectively. Vol; s and Vol; d are volume of LV at the end of systole and diastole, respectively. SV, stroke volume. CO, cardiac output. LVEF, LV ejection fraction. LVFS, LV fractional shortening. Data are mean ± SEM, *$P<0.05$, **$P<0.001$ vs. Sham + Ad-GFP. †$P<0.05$, ††$P<0.001$, vs. MI + Ad-GFP.

manuscript. **Qingping Feng:** conceived the experiments. designed the experiments. wrote the manuscript. revised the manuscript. All authors contributed to the interpretation of results and proofreading of the manuscript.

Declaration of competing interest

The authors declare that they have no known competing financial interests or personal relationships that could have appeared to influence the work reported in this paper.

Data availability

Data will be made available on request.

Acknowledgement

This work was supported by an operating grant from the Canadian Institutes of Health Research (CIHR) to QF and an Ontario Graduate Scholarship to JNB. QF holds a Richard and Jean Ivey Chair in Molecular Toxicology at Western University. This study was part of JNB's PhD thesis, which was posted on the Electronic Thesis and Dissertation Repository, Western University https://ir.lib.uwo.ca/etd/4897.

Appendix A. Supplementary data

Supplementary data to this article can be found online at https://doi.org/10.1016/j.ejphar.2022.175287.

References

Bax, N.A., van Oorschot, A.A., Maas, S., Braun, J., van Tuyn, J., de Vries, A.A., et al., 2011. In vitro epithelial-to-mesenchymal transformation in human adult epicardial cells is regulated by TGFbeta-signaling and WT1. Basic Res. Cardiol. 106, 829–847. https://doi.org/10.1007/s00395-011-0181-0.

Blom, J.N., Feng, Q., 2018. Cardiac repair by epicardial EMT: current targets and a potential role for the primary cilium. Pharmacol. Ther. 186, 114–129. https://doi.org/10.1016/j.pharmthera.2018.01.002.

Bodle, J.C., Loboa, E.G., 2016. Concise review: primary cilia: control centers for stem cell lineage specification and potential targets for cell-based therapies. Stem Cell. 34, 1445–1454. https://doi.org/10.1002/stem.2341.

Bui, A.L., Horwich, T.B., Fonarow, G.C., 2011. Epidemiology and risk profile of heart failure. Nat. Rev. Cardiol. 8, 30–41. https://doi.org/10.1038/nrcardio.2010.165.

Cook, C., Cole, G., Asaria, P., Jabbour, R., Francis, D.P., 2014. The annual global economic burden of heart failure. Int. J. Cardiol. 171, 368–376. https://doi.org/10.1016/j.ijcard.2013.12.028.

Diguet, N., Le Garrec, J.-F., Lucchesi, T., Meilhac, S.M., 2015. Imaging and analyzing primary cilia in cardiac cells. Methods Cell Biol. 127, 55–73. https://doi.org/10.1016/bs.mcb.2015.01.008.

Duan, J., Gherghe, C., Liu, D., Hamlett, E., Srikantha, L., Rodgers, L., et al., 2012. Wnt1/b-catenin injury response activates the epicardium and cardiac fibroblasts to promote cardiac repair. EMBO J. 31, 429–442. https://doi.org/10.1038/emboj.2011.418.

Egorova, A.D., Khedoe, P.P., Goumans, M.J., Yoder, B.K., Nauli, S.M., ten Dijke, P., et al., 2011. Lack of primary cilia primes shear-induced endothelial-to-mesenchymal transition. Circ. Res. 108, 1093–1101. https://doi.org/10.1161/CIRCRESAHA.110.231860.

Feng, Q., Lu, X., Jones, D.L., Shen, J., Arnold, J.M.O., 2001. Increased inducible nitric oxide synthase expression contributes to myocardial dysfunction and higher mortality post-myocardial infarction in mice. Circulation 104, 700–704.

Goetz, S.C., Anderson, K.V., 2010. The primary cilium: a signalling centre during vertebrate development. Nat. Rev. Genet. 11, 331–344. https://doi.org/10.1038/nrg2774.

Gonzalez, D.M., Medici, D., 2014. Signaling mechanisms of the epithelial-mesenchymal transition. Sci. Signal. 7, re8. https://doi.org/10.1126/scisignal.2005189.

Hassounah, N.B., Bunch, T.A., McDermott, K.M., 2012. Molecular pathways: the role of primary cilia in cancer progression and therapeutics with a focus on Hedgehog signaling. Clin. Cancer Res. : Off. J.Am. Assoc. Cancer Research 18, 2429–2435. https://doi.org/10.1158/1078-0432.CCR-11-0755.

Jing, X., Gao, Y., Xiao, S., Qin, Q., Wei, X., Yan, Y., et al., 2016. Hypoxia induced the differentiation of Tbx18-positive epicardial cells to CoSMCs. Sci. Rep. 6, 30468 https://doi.org/10.1038/srep30468.

Kim, J., Wu, Q., Zhang, Y., Wiens, K.M., Huang, Y., Rubin, N., et al., 2010. PDGF signaling is required for epicardial function and blood vessel formation in regenerating zebrafish hearts. Proc. Natl. Acad. Sci. U. S. A. 107, 17206–17210. https://doi.org/10.1073/pnas.0915016107.

Lancaster, M.A., Schroth, J., Gleeson, J.G., 2011. Subcellular spatial regulation of canonical Wnt signalling at the primary cilium. Nat. Cell Biol. 13, 700–707. https://doi.org/10.1038/ncb2259.

Lencinas, A., Tavares, A.L.P., Barnett, J.V., Runyan, R.B., 2011. Collagen gel analysis of epithelial-mesenchymal transition in the embryo heart: an in vitro model system for the analysis of tissue interaction, signal transduction, and environmental effects. Birth Defects Res. C Embryo Today 93, 298–311. https://doi.org/10.1002/bdrc.20222.

Li, Y., Klena, N.T., Gabriel, G.C., Liu, X., Kim, A.J., Lemke, K., et al., 2015. Global genetic analysis in mice unveils central role for cilia in congenital heart disease. Nature 521, 520–524. https://doi.org/10.1038/nature14269.

Liu, Y., Lu, X., Xiang, F.L., Poelmann, R.E., Gittenberger-de Groot, A.C., Robbins, J., et al., 2014. Nitric oxide synthase-3 deficiency results in hypoplastic coronary arteries and postnatal myocardial infarction. Eur. Heart J. 35, 920–931. https://doi.org/10.1093/eurheartj/ehs306.

Moazzen, H., Lu, X., Liu, M., Feng, Q., 2015. Pregestational diabetes induces fetal coronary artery malformation via reactive oxygen species signaling. Diabetes 64, 1431–1443. https://doi.org/10.2337/db14-019.

Moazzen, H., Wu, Y., Engineer, A., Lu, X., Aulakh, S., Feng, Q., 2020. NOX2 is critical to endocardial to mesenchymal transition and heart development. Oxid. Med. Cell. Longev. 2020, 1679045 https://doi.org/10.1155/2020/1679045.

Murdoch, C.E., Chaubey, S., Zeng, L., Yu, B., Ivetic, A., Walker, S.J., et al., 2014. Endothelial NADPH oxidase-2 promotes interstitial cardiac fibrosis and diastolic dysfunction through proinflammatory effects and endothelial-mesenchymal transition. J. Am. Coll. Cardiol. 63, 2734–2741. https://doi.org/10.1016/j.jacc.2014.02.572.

Myklebust, R., Engedal, H., Saetersdal, T.S., Ulstein, M., 1977. Primary 9 + 0 cilia in the embryonic and the adult human heart. Anat. Embryol. 151, 127–139. https://doi.org/10.1007/BF00297476.

Ott, C., Lippincott-Schwartz, J., 2012. Visualization of live primary cilia dynamics using fluorescence microscopy. Curr Protoc Cell Biol Chapter 4. https://doi.org/10.1002/0471143030.cb0426s57. Unit 4.26.

Pazour, G.J., Dickert, B.L., Vucica, Y., Seeley, E.S., Rosenbaum, J.L., Witman, G.B., et al., 2000. Chlamydomonas IFT88 and its mouse homologue, polycystic kidney disease gene tg737, are required for assembly of cilia and flagella. J. Cell Biol. 151, 709–718.

Perez-Pomares, J.M., de la Pompa, J.L., 2011. Signaling during epicardium and coronary vessel development. Circ. Res. 109, 1429–1442. https://doi.org/10.1161/CIRCRESAHA.111.245589.

Plotnikova, O.V., Pugacheva, E.N., Golemis, E.A., 2009. Primary cilia and the cell cycle. Methods Cell Biol. 94, 137–160. https://doi.org/10.1016/S0091-679X(08)94007-3.

Potts, J.D., Runyan, R.B., 1989. Epithelial-mesenchymal cell transformation in the embryonic heart can be mediated, in part, by transforming growth factor beta. Dev. Biol. 134, 392–401.

Rozycki, M., Lodyga, M., Lam, J., Miranda, M.Z., Fatyol, K., Speight, P., et al., 2014. The fate of the primary cilium during myofibroblast transition. Mol. Biol. Cell 25, 643–657. https://doi.org/10.1091/mbc.E13-07-0429.

Sanchez-Duffhues, G., de Vinuesa, A.G., Lindeman, J.H., Mulder-Stapel, A., DeRuiter, M. C., Van Munsteren, C., et al., 2015. SLUG is expressed in endothelial cells lacking primary cilia to promote cellular calcification. Arterioscler. Thromb. Vasc. Biol. 35, 616–627. https://doi.org/10.1161/ATVBAHA.115.305268.

Shenje, L.T., Andersen, P., Halushka, M.K., Lui, C., Fernandez, L., Collin, G.B., et al., 2014. Mutations in Alstrom protein impair terminal differentiation of cardiomyocytes. Nat. Commun. 5, 3416. https://doi.org/10.1038/ncomms4416.

Slough, J., Cooney, L., Brueckner, M., 2008. Monocilia in the embryonic mouse heart suggest a direct role for cilia in cardiac morphogenesis. Dev. Dynam. : Off. Pub. Am. Assoc. Anatom. 237, 2304–2314. https://doi.org/10.1002/dvdy.21669.

Smart, N., Dube, K.N., Riley, P.R., 2013. Epicardial progenitor cells in cardiac regeneration and neovascularisation. Vasc. Pharmacol. 58, 164–173. https://doi.org/10.1016/j.vph.2012.08.001.

Takeichi, M., Nimura, K., Mori, M., Nakagami, H., Kaneda, Y., 2013. The transcription factors Tbx18 and Wt1 control the epicardial epithelial-mesenchymal transition through bi-directional regulation of Slug in murine primary epicardial cells. PLoS One 8, e57829. https://doi.org/10.1371/journal.pone.0057829.

Tao, J., Doughman, Y., Yang, K., Ramirez-Bergeron, D., Watanabe, M., 2013. Epicardial HIF signaling regulates vascular precursor cell invasion into the myocardium. Dev. Biol. 376, 136–149. https://doi.org/10.1016/j.ydbio.2013.01.026.

Valenta, T., Hausmann, G., Basler, K., 2012. The many faces and functions of b-catenin. EMBO J. 31, 2714–2736. https://doi.org/10.1038/emboj.2012.150.

Villalobos, E., Criollo, A., Schiattarella, G.G., Altamirano, F., French, K.M., May, H.I., et al., 2019. Fibroblast primary cilia are required for cardiac fibrosis. Circulation 139, 2342–2357. https://doi.org/10.1161/CIRCULATIONAHA.117.028752.

von Gise, A., Pu, W.T., 2012. Endocardial and epicardial epithelial to mesenchymal transitions in heart development and disease. Circ. Res. 110, 1628–1645. https://doi.org/10.1161/CIRCRESAHA.111.259960.

Wang, J., Cao, J., Dickson, A.L., Poss, K.D., 2015. Epicardial regeneration is guided by cardiac outflow tract and Hedgehog signalling. Nature 522, 226–230. https://doi.org/10.1038/nature14325.

Xiang, F.L., Liu, Y., Lu, X., Jones, D.L., Feng, Q., 2014. Cardiac-specific overexpression of human stem cell factor promotes epicardial activation and arteriogenesis after myocardial infarction. Circ Heart Fail 7, 831–842. https://doi.org/10.1161/CIRCHEARTFAILURE.114.001423.

Xiang, F.L., Lu, X., Hammoud, L., Zhu, P., Chidiac, P., Robbins, J., et al., 2009. Cardiomyocyte-specific overexpression of human stem cell factor improves cardiac function and survival post myocardial infarction in mice. Circulation 120, 1065–1074.

Zebrowski, D.C., Vergarajauregui, S., Wu, C.-C., Piatkowski, T., Becker, R., Leone, M., et al., 2015. Developmental alterations in centrosome integrity contribute to the post-mitotic state of mammalian cardiomyocytes. Elife 4. https://doi.org/10.7554/eLife.05563.

Zhou, B., Honor, L.B., He, H., Ma, Q., Oh, J.H., Butterfield, C., et al., 2011. Adult mouse epicardium modulates myocardial injury by secreting paracrine factors. J. Clin. Invest. 121, 1894–1904. https://doi.org/10.1172/JCI45529.